Absorption spectroscopy and photodissociation dynamics of small helium cluster ions

H. Haberland and B. v. Issendorff[a)]
Fakultät für Physik, Universität Freiburg, H. Herderstr. 3, D-79104 Freiburg, Germany

R. Fröchtenicht[b),c)] and J. P. Toennies
Max-Planck-Institut für Strömungsforschung, Bunsenstrasse 10, D-37073 Göttingen, Germany

(Received 15 December 1994; accepted 23 February 1995)

The optical absorption of size-selected helium cluster ions was studied via photofragmentation spectroscopy. Absorption cross sections were measured for He_n^+ ($n=3$, 4, 10, 21, and 30). A broad absorption peak was found, which for He_3^+ is centered at ≈ 5.3 eV, and which with increasing cluster size shifts slightly to the red. In addition, the kinetic energy release to the ionized and neutral photofragments was measured by a time-of-flight technique for cluster sizes between $n=3$ and 10. From the energy balance the total binding energy of the He_3^+ trimer ion was determined to be 2.6 ± 0.15 eV. The results further indicate that a charged linear trimer acts as a core molecule for the sizes $n=4-7$. For $n>7$, an additional isomer with a tetramer core is identified. The results are compared with recent *ab initio* calculations. © *1995 American Institute of Physics.*

I. INTRODUCTION

Helium cluster ions are among the simplest of the growing number of cluster ions which have attracted increasing attention in recent years.[1] Since for a simple linear combination of atomic orbitals (LCAO) description of their lowest electronical states only the atomic 1*s* orbitals have to be taken into account, a very restricted number of states arise, which makes these clusters ideal model systems for the study of charge delocalization and geometry effects. Despite their simplicity not much experimental work has been done on He cluster ions up to now. Maas *et al.*[2] determined a value of $D_e=2.475$ eV for the binding energy of He_2^+ in a combined experimental and theoretical study, and Patterson[3] measured a binding energy of $D_0=0.17$ eV for He_3^+. Besides these two experiments there is mainly the work of Toennies and coworkers, who measured mass spectra[4] and appearance potentials[5] in electron impact studies of neutral He clusters. In a recent experiment the photoionization dynamics of neutral He clusters were also studied by using synchrotron excitation.[6]

A number of groups have performed quantum chemical calculations on the geometric as well as electronic properties of the small cluster ions.[2,7–12] A rather consistent picture emerges from these studies. For He_2^+ a binding energy of $D_e=2.4-2.5$ eV (Refs. 8, 10, and 11) and a bond length of 1.08 Å was determined. The trimer was calculated to be a linear symmetric molecule with a bond length of 1.24 Å and a binding energy of $D_e=0.15-0.17$ eV.[8,9,11] For the cluster sizes $n=4-7$ the calculations predict that the trimer acts as an ionized core with further atoms being attached to it in an equatorial position at a distance of 2.3 Å.[8,10] Each of these atoms is then rather weakly bound by polarization forces with a binding energy of $D_e=0.03$ eV. It was further established that these geometric structures can only be explained if electron correlation is properly taken into account. Without correlation the calculations predict that the charge tends to localize on the dimer core.[8,10] Staemmler has also calculated the excitation energies for some fixed geometries of He_n^+ ($n=2-7$).[12] For the optically allowed transitions of the dimer, trimer, and a linear symmetric tetramer he determined energies of 9.9, 5.5, and 5.0 eV, respectively.

In this article we present the first spectroscopic study of helium cluster ions. These experiments supplement similar work carried out by Haberland and co-workers on ionized argon and xenon clusters, which include the determination of photoabsorption cross sections[13] and recently measurements of photofragment kinetic energies. In these systems the positive charge tends to localize on a linear trimer, but also strong evidence for the at least transient formation of a tetramer core structure was found.[14]

The present report starts with a description of the experimental techniques. It continues with a presentation of the measured photoabsorption cross sections and the observed product time-of-flight spectra, and ends with a discussion of the conclusions which can be drawn from the data. This paper is intended to focus on the properties of the small ionized helium clusters in the electronic ground state. In a separate publication[15] we report on a related study demonstrating that certain anomalous characteristics of He_4^+ which can be observed under special source conditions are due to a metastable electronical excitation.

II. EXPERIMENT

The photoabsorption measurements were performed in a double time-of-flight mass spectrometer (TOF-MS), which has already been described in detail.[16] The arrangement is shown schematically in Fig. 1. Briefly, neutral helium clusters were produced by a low temperature supersonic expansion (source diameter 5 μm, source temperature $T_0=8-20$ K, stagnation pressure $P_0=50$ bar). The construction of the cryostat and the nozzle are described in Refs. 4 and 5. After passing a 0.8 mm diam skimmer, the clusters were ionized

[a)]E-mail: bernd@frha06.physik.uni-freiburg.de
[b)]E-mail: froechtenich@msfd1.dnet.gwdg.de
[c)]Present address: BMW AG, D-80788 München, Germany.

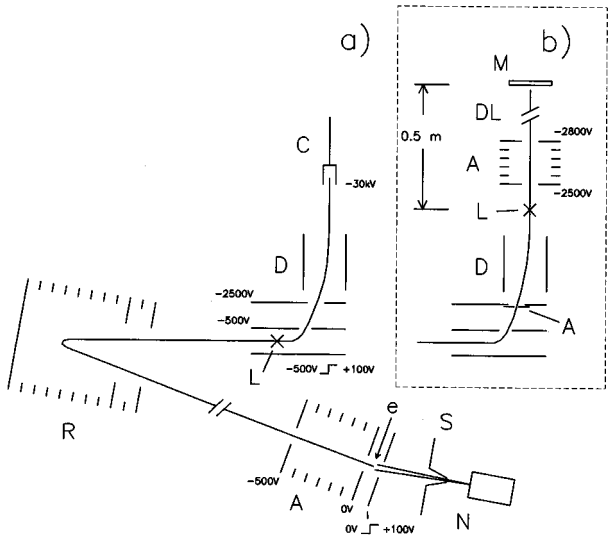

FIG. 1. Schematic diagram of the apparatus. The primary time-of-flight mass spectrometer consists of the nozzle (N), skimmer (S), electron beam (e), accelerator (A), and reflector (R). Two types of secondary TOF-MS are used: Type (a) for measurements of photoabsorption cross sections consists of a Wiley–McLaren accelerator with laser interaction region (L), deflection plates (D), and a conversion dynode detector (C); type (b) for measurements of the fragment kinetic energies consists of the same accelerator with aperture (A), laser interaction region (L), accelerator (A), drift region (DL), and a multichannelplate detector (M). Typical voltages are indicated.

by an electron beam of 200 eV energy and then accelerated to 600 eV into a reflectron TOF-MS. Behind the reflector in the spatial focus of the reflectron ions of a given mass were irradiated by laser pulses from a frequency doubled dye-laser (Lambda Physik excimer pumped dye laser with BBOI/BBOII crystals pulse duration $\approx$10 ns) at a selected wavelength between $\lambda=210$–300 nm and subsequently extracted into a second linear TOF-MS. At the end of a drift region the ions were then detected by a modified Daly detector, the signal of which is recorded with a fast transient recorder (100 MHz, 8 bit). In this second spectrometer clusters which were dissociated after absorption of a photon were separated from unfragmented clusters. The decrease of the original cluster intensity produced by the laser excitation together with the monitored laser intensity yields the absolute photofragmentation cross section. For the bound-free transitions considered here, this photofragmentation cross section is equal to the photoabsorption cross section.

Because of the low intensity of the frequency doubled laser light and the small absorption cross sections involved, the ratio of dissociated to undissociated clusters was less than 10% even in the maximum of the absorption. This led to a large statistical error in the cross sections and ultimately to a modification of the experiment. Instead of monitoring the cluster signal depletion for determining the profile of the absorption, the appearance of the cluster fragments as a function of the laser frequency was measured. This is more favorable, since a rise of a small signal on a negligible background can be detected with a significantly smaller statistical error than a small depletion on a large signal. This method, however, only yields relative absorption cross sections. The obtained absorption profiles therefore were scaled to the absolute values measured by the depletion technique in the absorption maximum.

For the measurement of the product kinetic energy release the second TOF-MS was modified [cf. Fig. 1(b)]. In principle, it is a linear Wiley–McLaren type TOF-MS located at the focus point of the reflectron perpendicularly to the beam axis of the first mass spectrometer. Preselected cluster ions are deflected into the second spectrometer by a high voltage pulse applied to the first stage of a two stage accelerator. Behind the accelerator the cluster beam is bent by electrostatic deflection plates into a direction perpendicular to the beam axis of the first TOF-MS. After passing a drift length of 0.5 m the cluster ions ($E\approx3000$ eV) are detected on a multichannel plate (MCP). In contrast to the absorption measurements described earlier, here a polarized laser pulse crosses the beam behind the two stages of the Wiley–McLaren accelerator and the deflection plates at the beginning of the drift region. The center-of-mass velocity of the cluster fragments gained in the dissociation process will thus lead to a splitting of the TOF peaks. In order to separate fragments of different masses, an acceleration field is placed behind the laser interaction zone, which is weak enough (potential difference of 10% to 20% of the cluster ion kinetic energy) not to affect the temporal resolution of the TOF setup. Not only ionized but also neutral fragments are detected since both have kinetic energies of several hundred volts, stemming from cluster ions with a kinetic energy of about 3000 V. With this arrangement it is thus possible to simultaneously measure the velocity distributions of all fragments (ionized and neutral) in one spectrum. The measured flight times are very reliable since scattered light from the laser pulse produces a signal on the MCP, which serves as an exact time fiduciary mark. Therefore no delay times of preamplifiers or trigger lines have to be account for.

III. RESULTS

The measured photoabsorption cross sections are displayed in Fig. 2 as a function of the laser photon energy for He_3^+, He_4^+, He_{10}^+, He_{21}^+, and He_{30}^+. The single peak seen in each of the spectra was fitted by a Gaussian profile. The resulting peak positions, widths, and maxima are summarized in Table I. Unfortunately, the maximum of the absorption lies close to the upper limit of the frequency-doubled laser frequency of 5.9 eV, so that only the low energy side of the peak could be measured adequately. For this reason the actual errors of the fit parameters given in Table I are chosen larger than the statistical ones calculated by the fit procedure.

As seen in Fig. 2 the absorption peak does not change much with cluster size. Its position exhibits a small, but significant red shift with increasing size. The apparent slight increase of the cross section seen in Table I and Fig. 2 probably is not significant since it lies within the experimental error. These results will be discussed in Sec. IV.

Examples of fragment time-of-flight spectra measured with the configuration shown in Fig. 1(b) are displayed in Fig. 3. The product signal is plotted as a function of the flight time after photodissociation of He_n^+ ($n=3$–5) at a laser wavelength of 225 nm (5.51 eV). The laser light was polar-

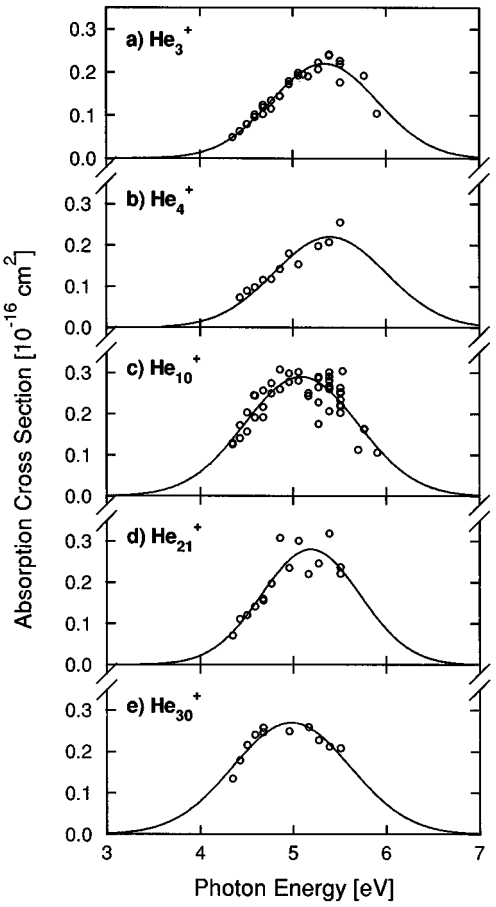

FIG. 2. Measured photoabsorption cross sections (○) as a function of the laser excitation energy for (a) He_3^+, (b) He_4^+, (c) He_{10}^+, (d) He_{21}^+, and (e) He_{30}^+ together with a Gaussian fit (—) to the data. The resulting fit parameters are summarized in Table I.

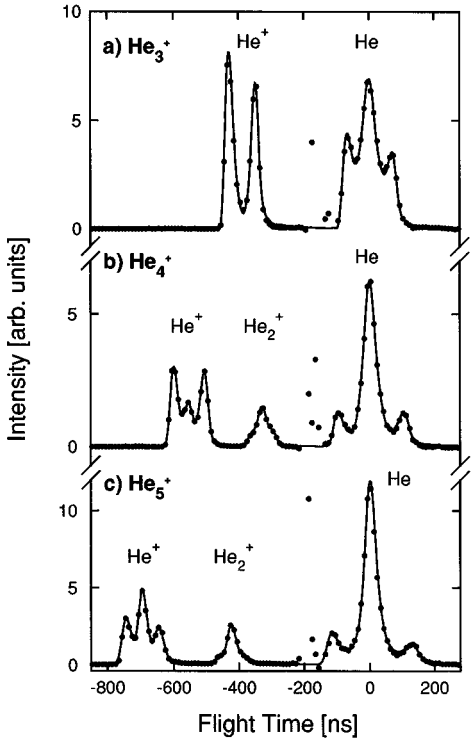

FIG. 3. Time-of-flight spectra of the photofragments after dissociation of (a) He_3^+, (b) He_4^+, and (c) He_5^+ at 225 nm with the laser light polarized parallel to the beam axis. From left to right the peaks correspond to the photofragments He^+, He_2^+, and neutral He atoms, respectively. The peaks of the unfragmented clusters have been suppressed by subtracting spectra recorded without laser excitation. Therefore, only a noiselike structure is visible at the position where parent cluster peak would appear, which is due to statistical fluctuations of the peak.

ized parallel to the cluster beam axis, as it was in all of the other measurements reported here. The flight time of the unfragmented ("parent") cluster ions was chosen as time zero. This parent cluster peak has a much higher intensity than the fragment peaks and, therefore, has been suppressed in the results of Fig. 3 by subtracting a spectrum measured without laser excitation. Therefore, only a noiselike structure is visible at the position where it would appear, which is due to statistical fluctuations of the peak.

The sequence of the arrival times of the different fragments can be explained as follows. After photofragmentation both the parent cluster ions and the fragments have nearly the same velocity in the laboratory system. In the static field behind the laser interaction region the ions are accelerated to velocities which depend on their e/m ratio, whereas the neutral He atoms do not experience a change in speed. Therefore, in the time-of-flight spectra, He^+ arrives before He_2^+, which arrives prior to He_3^+, and so on. The last fragments to arrive are the neutrals.

As can be seen in Fig. 3 the TOF peaks corresponding to the different cluster ion photofragments exhibit a similar structure. The respective central peak is attributed to particles which have not gained large center-of-mass velocities in the course of the photofragmentation. The wings at both sides are attributed to fragments with velocity vectors which in the center-of-mass system are either parallel or antiparallel to the beam direction. These wings are unequal in height for three reasons: First, because of the Jacobian arising in the transformation of velocity to flight time ($dv \propto t^{-2} dt$), second, because of the finite detector solid angle, and third due to the velocity dependent detection probability of the MCP which increases with increasing velocity.

Similar time-of-flight spectra were measured for cluster ions with sizes $n=3$–10 at three different excitation wavelengths (225, 250, and 270 nm). In addition, by electrostatically suppressing all ionized particles, the neutral fragments were isolated in order to get spectra without the disturbing

TABLE I. Positions, widths, and maxima of the absorption cross sections determined from Gaussian fits to the absorption profiles shown in Fig. 2 for different He cluster ions.

Cluster ion	Position (eV)	Width (eV)	Max. cross section (10^{-16} cm^2)
He_3^+	5.34	0.57	0.22
He_4^+	5.40	0.6	0.22
He_{10}^+	5.09	0.61	0.29
He_{21}^+	5.19	0.53	0.28
He_{30}^+	4.98	0.63	0.27
Error	−0.1/+0.2	−0.05/+0.1	−0.1/+0.2

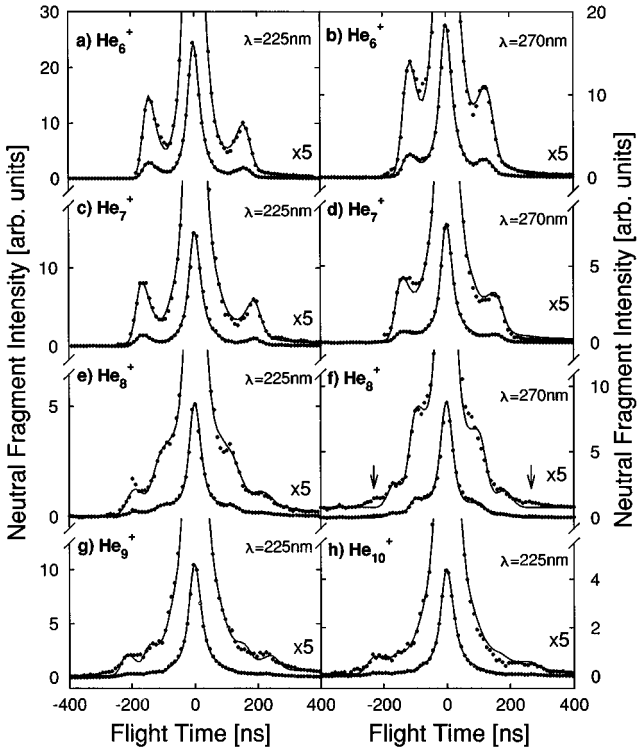

FIG. 4. Time-of-flight spectra of the neutral fragments after photodissociation of He_n^+ ($n=6-10$) at 225 and 270 nm with the laser light polarized parallel to the beam axis. The solid line represents the result of a fit with model functions. The small outermost pair of wings appearing at 270 nm has not been fitted here for better visibility.

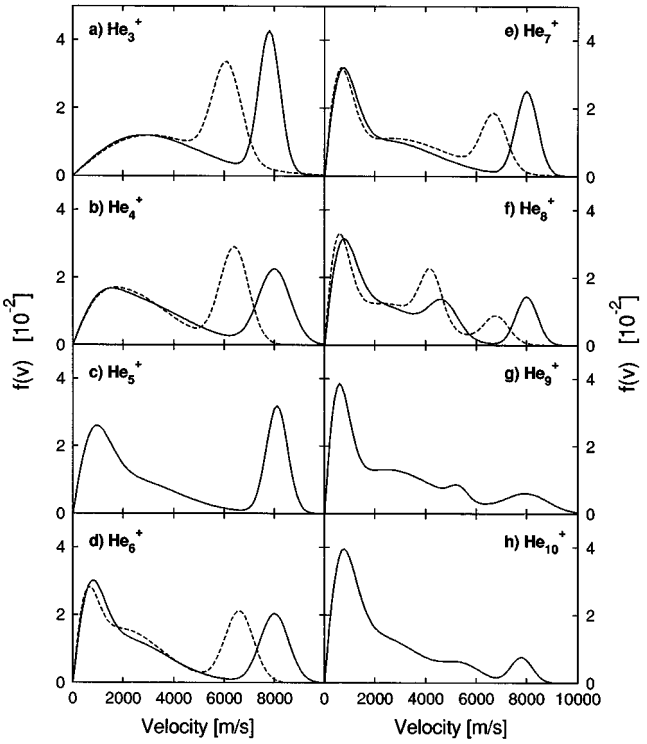

FIG. 5. Deconvoluted center-of-mass velocity distributions of the neutral fragments, $f(v)$, obtained from the experimental data in Fig. 4. The solid line refers to an excitation wavelength of 225 nm (5.5 eV); the dashed line to 270 nm (4.6 eV).

peaks of the unfragmented parent cluster ions. Examples for the neutral fragment spectra are displayed in Fig. 4. For He_7^+ and He_8^+ only the neutral spectra could be measured due to a high background intensity of nitrogen and oxygen molecular ions at mass 28 and 32 amu, respectively. Although their abundance in the beam was up to four times higher than that of He_7^+ or He_8^+, they do not contribute to the measured spectra of the neutral fragments, since they are not dissociated [$D_0=8.71$ eV for N_2^+ and 6.66 eV for O_2^+ (Ref. 17)] at the photon energies used.

The TOF spectra were fitted with simple model functions. For the fast and the slow fragments two different types of distributions were used. The fast particles were assumed to have a $\cos^2\theta$ angular distribution with respect to the laser polarization, as can be expected for the fragmentation of a linear chromophore with a parallel transition moment.[18] The absolute value of their velocities v was modeled with a Gaussian distribution:

$$f_f(v,\theta)\propto\cos^2(\theta)\exp\left(-\frac{(v-v_0)^2}{2\sigma^2}\right). \tag{1}$$

For the slow particles the best fit was achieved with an isotropic Boltzmann-like velocity distribution:

$$f_s(v,\theta)\propto v\ \exp\left(-\frac{v^2}{2\sigma^2}\right). \tag{2}$$

This distribution describes the motion of those particles which do not experience a direct repulsion in the excited state. Examples are the central atom in the charged trimer or the atoms which are located in the ring around the trimer core. For the fit of this slow component in the neutral velocity distribution sometimes two f_s distributions with different widths σ were used. The finite solid angle of the MCP and the measured temporal resolution of the spectrometer were taken into account via a Monte Carlo convolution.[19] The velocity distributions for the neutral fragments which were used to fit the measured data in Fig. 4 are shown in Fig. 5 for the wavelengths 225 nm (—) and 270 nm (---). The relative intensities of the slow and fast He_1^+ and He_2^+ fragments are listed in Table II.

The trimer ion fragmentation spectra were additionally fitted in a different way. In order to obtain a reliable value for the binding energy of the trimer the velocities of the fast and the slow particles were not fitted with two independent distributions. Instead a distribution similar to Eq. (2) was used for the central particle whereas the velocities of the outer particles were calculated from the conservation of energy and momentum. It was also assumed that the outer particles have equal velocity components perpendicular to the axis defined by the transition moment, and that the central particle is ejected mainly perpendicularly to this axis.[19] Taking all this into account the outer peaks could be fitted with only two free parameters: their amplitude and the total kinetic energy.

From the two spectra measured at 225 nm (5.51 eV) and 270 nm (4.59 eV), total kinetic energies of 2.92 and 1.96 eV were obtained, yielding total binding energies of 2.59 and 2.63 eV,

TABLE II. Deconvoluted relative intensities of the ionic products for different cluster ions and two excitation wavelengths λ.

Cluster ion	λ (nm)	Relative intensities of the product ions (%)			
		He_1^+ slow	He_1^+ fast	He_2^+ slow	He_2^+ fast
He_3^+	225	100	0	0	0
	270	100	0	0	0
He_4^+	225	69	11	7	13
	270	55	13	25	7
He_5^+	225	52	26	7	15
	270	36	21	18	25
He_6^+	225	35	25	6	34
	270	23	16	29	32
He_9^+	225	6	13	32	49
He_{10}^+	225	8	9	31	52
	270	4	1	48	47

respectively. Thus we can determine for the total binding energy of He_3^+ a value of $D_0=2.6\pm0.15$ eV. The error is estimated from the uncertainties in the evaluation procedure.

IV. DISCUSSION

A. He_3^+

As with the other ionized rare gas clusters it is interesting to establish on what entity within the helium cluster ion the positive charge is localized. Clusters with a dimer ion core should have an absorption spectrum similar to that of a free dimer ion, i.e., an absorption maximum near the lowest excitation energy of the dimer, for which a value of about 10 eV has been calculated.[12] The position of the He_3^+ maximum absorption at 5.34 eV determined in this work, however, agrees quite well with the calculated value of 5.5 eV for a symmetric linear trimer ion.[12] This suggests that the He_3^+ molecular ion has this geometric structure with the charge being delocalized over all three atoms. It should be noted, however, that from the present experimental data the existence of an additional isomer, consisting of a dimer ion core with a loosely attached neutral He atom, cannot be ruled out. The absorption of such a species lies outside the examined wavelength region. With the present setup this could only be excluded if the laser intensity and the cross sections were large enough so as to be sure that all clusters are fragmented and thereby rule out the existence of an additional nonabsorbing species. In view of the theoretical results, however, such a configuration seems rather unlikely, although not impossible.

The product time-of-flight spectra show that He_3^+ dissociates into one fast neutral He atom, one fast He^+ ion and another slow neutral atom (cf. Fig. 3). This pattern can easily be understood by examining the orbitals of the excited state. Figure 6 schematically shows the three possible states of the symmetric linear He_3^+. In Fig. 6(a) the three possible molecular orbitals are shown, which can be formed out of the atomic *s* orbitals. As usual, the sign of each wave function is indicated by the shading of the circles and its amplitude by their radii. Filling these molecular orbitals with the five available electrons three molecular states arise. In each of these states one of the three molecular orbitals is only filled with one electron. This half filled orbital determines the spatial distribution of the positive charge. Thus the three electronic states of the trimer can alternatively be described as three hole states with respective wavefunctions, as indicated in Fig. 3(b). The only allowed optical transition is $\Sigma_g \rightarrow \Sigma_u$. The excited Σ_u state is totally repulsive, because in this state there are two electrons in the bonding and also two electrons in the more strongly antibonding orbital, whereas the one electron in the nonbonding σ_u orbital has no influence. Since in this state the hole has zero probability to be located in the middle, only the outer atoms can accommodate the positive charge. If this charge distribution is maintained during fragmentation, a trimer in the Σ_u state will thus dissociate into one slow neutral and two fast particles which are ejected with equal momentum to both sides, one of them carrying the charge as observed in the experiment.

The charge distribution after the fragmentation is an interesting point. In the case of photodissociation of an argon

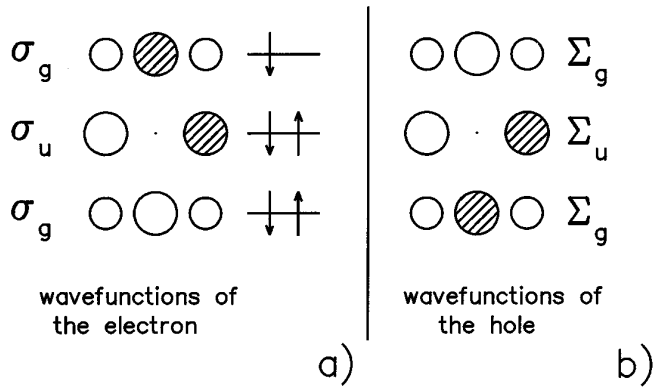

FIG. 6. The lowest electronic states of linear symmetric He_3^+ in a simple LCAO picture. Three molecular orbitals arise from the linear combination of the helium atomic *s* orbitals (a); radius and shading of the circles indicate magnitude and sign of the coefficients with which the *s* orbitals enter the different linear combinations. Filling these with the five electrons of the He_3^+, three possible states result, which are shown in (b). The distribution of the positive charge in each of these states is determined by the wave function of the respective half-filled orbital. Note that in the optically active state Σ_u (all orbitals filled with two electrons except the σ_u orbital) the positive charge has a vanishing probability to be located on the middle atom.

trimer, in addition to fast monomer ion fragments, slow ions are also observed.[20,21] The latter were explained by nonadiabatic transitions between states of different symmetry during breakup at larger internuclear distances.[22] Since for He_3^+ no slow ion fragments could be observed (detection limit of less than 2% of the fast ion signal), it follows that such a nonadiabatic transition does not take place here.

Another interesting feature in the He_3^+ TOF spectrum is the relative broadness of the central peak of the neutral fragments. It indicates a relatively high average recoil velocity of the middle atom, which reaches values of more than half of the velocity of the outer atoms. Such a high velocity of the middle particle is not allowed in the case of fragmentation of a rigidly linear molecule,[23] but can be explained by accounting for the vibrational bending mode of the trimer. If the electronic transition occurs when the trimer is bent, the central particle will gain considerable momentum perpendicular to the molecular axis. At the classical turning point of the ground vibrational level of the bending mode, which corresponds to an opening angle of about 160° [deduced from the calculated frequency of 260 cm^{-1} (Ref. 6)], the central atom already obtains more than 35% of the velocity of the outer particles. Therefore the broadness of the central peak indicates that He_3^+ is a very floppy molecule with respect to bending. This is not astonishing since the molecular orbitals consist of atomic *s* orbitals and thus do not provide strong alignment forces.

B. He_4^+

The photoabsorption spectrum of He_4^+ [cf. Fig. 2(b)], as well as its fragment TOF spectra [cf. Fig. 3(b)], are quite similar to those of He_3^+. This suggests that the tetramer ion indeed consists of a trimer ion core with a loosely attached additional neutral atom bound by polarization forces. The small differences in the fragment TOF spectra include a higher intensity of the slow neutral fragments and the appearance of slow monomer ions and ionized dimers in the case of the tetramer ion. The higher intensity of slow neutrals is due to the fact that there are now two He atoms, the central particle of the linear trimer core and the neutral atom attached to the trimer, which do not experience a strong repulsion in the course of the dissociation. The appearance of slow ions and of dimer ions can be explained by the breaking of the symmetry by the attached neutral atom. In the excited state, which can now only approximately be described by the Σ_u state of the trimer core, the localization of some charge on the middle atom as well as on the attached atom becomes allowed, thus opening up channels for fragmentation with a remaining slow ion.

Surprisingly, the dimer fragment exhibits a TOF structure with a central peak of slow particles ($<$3000 m/s) and two shoulders of fast ones (about 4000 m/s). The slow dimer ions can only be formed out of the middle particle of the trimer core and the former attached neutral atom. They cannot be produced by fragmentation of the trimer ion core into a slow ionized dimer and a correspondingly slow neutral monomer since, in that case because of the low kinetic energy of the products, conservation of energy could not be fulfilled. The high photon energy and the estimated low total binding energy of the cluster of about 2.63 eV require the production of fragments with a greater kinetic energy.

The origin of the fast dimers is more difficult to understand. Energy conservation does not exclude that they are produced by a fragmentation of the trimer core into a dimer ion and a fast He atom. This seems very unlikely, however, since the excited state is totally repulsive. A more likely explanation is the fragmentation of a linear tetramer, the excited state of which dissociates into two dimers, a charged one and an unbound neutral one. This would suggest that even the He_4^+ ion can have a linear structure at least for short times, thus supporting the picture of a charged trimer with a neutral atom moving almost freely around it rather than the picture of a rigid T-shaped tetramer.

C. Larger cluster ions

From He_4^+ to He_7^+ the fragmentation patterns remain nearly the same. Only the ratios of slow to fast monomer ions and of monomer to dimer ionized fragments increase slowly. Between He_7^+ and He_8^+, however, the neutral fragment peak form changes from a single to a double wing structure [cf. Figs. 4(e) and 4(f)]. At a wavelength of 225 nm, these additional wings indicate particles with velocities of about 5000 m/s (0.52 eV for an He atom) for $\lambda = 225$ nm. If these particles were single atoms ejected to one side during the fragmentation, again the energy balance could not be satisfied, since the outer wings carry a total kinetic energy of about 2.7 eV (for $\lambda = 225$ nm). Since there is no additional degree of freedom to store energy in, the same amount of kinetic energy must be released in the process leading to the slow wings. The only possible process for a generation of the neutrals in the slow wings is either the dissociation of the core molecule into a fast monomer and an ionized dimer, which subsequently breaks up as well, or the dissociation into two dimers, one of which is ionized. The former can be excluded, since no fast neutrals with a velocity of about 10 000 m/s and an intensity equal to that of the slow wings could be detected. Fast dimers of 5000 m/s, however, could be observed for He_9^+ and He_{10}^+ in support of the latter mechanism, i.e., a fragmentation into two dimers. This is exactly what happens in the excited state of a symmetric linear tetramer. We conclude, therefore, that for He_8^+ and larger ions there is an isomer with a tetramer ion core in addition to the one with the trimer ion core. The outermost wings in the TOF peak of the neutral fragments are identical with the wings of the smaller clusters suggesting that they are due to the fragmentation of the isomer with the trimer ion core. The appearance of a tetramer ion core coincidences with the observed shift in the absorption spectrum, which at an ion cluster size of $n = 10$, is already close to the calculated value for a tetramer chromophore absorption.[12] Unfortunately, the trimer and tetramer peaks cannot be separated due to the broad absorption profile and the close positions of the maxima. A similar shift in the absorption position towards the red to a tetramer ion core can also be found in the fragmentation pattern of He_8^+: the ratio of the intensities of the inner wings to the outer wings increases with increasing wavelength [cf. Figs. 4(e) and 4(f)].

This appearance of a tetramer ion core for cluster ions larger than He_7^+ suggests that He_7^+ indeed has the very symmetrical structure of a trimer core with an equatorial ring of four atoms, as predicted both by Rosi and Bauschlicher[8] and Staemmler.[12] Since the structure provides no space in the filled ring of neutral atoms for an additional He atom, the position of this atom will be near one of the ends of the trimer core, thus giving rise to the at least transient formation of a tetramer ion core. One would expect that for sizes $\leqslant 7$, only the fragmentation pattern of a trimer core appears, while for bigger clusters, that of a tetramer core should appear which is exactly what we have observed. It must be noted that the appearance of a tetramer core fragmentation pattern does not require the existence of a stable isomer with a tetramer core. Since calculations indicate only a very small potential energy difference between structures with a trimer and a tetramer core and also a very small barrier between them, clusters like He_8^+ will probably not have either of the structures, but will rather oscillate between both.

In the neutral He atom product TOF spectra in Fig. 4 for all ion cluster sizes from $n=6$ to 10 at 270 nm (4.59 eV), a small pair of wings of very fast neutrals with velocities of about 10 000 m/s ($\approx$2.1 eV) can be seen which are indicated in Fig. 4(f) by arrows. The fits of these wings are not shown for better visibility. Two photon absorption can be excluded as an explanation for these fast atoms since their intensity shows a linear dependence on the laser intensity. This implies that the corresponding ionized fragment has to be a bound dimer ion because the energy of the one photon is not high enough to provide the measured kinetic energy as well as the total binding energy. The photon energy is 4.59 eV, and if a dimer ion is ejected with equal momentum to the very fast neutral, it will have a kinetic energy of $\approx$1 eV, so that the total kinetic energy of the dimer and the neutral fragment is $\approx$3 eV. The remaining energy of 1.6 eV is not enough to dissociate the dimer ($D_0=2.4$ eV). Therefore, we must assume that a vibrationally excited dimer ion in the electronic ground state is produced. This dissociation behavior can only be explained by assuming a crossing of an electronically excited state back to the ground state. One possible process where this can happen is an excitation involving a charge transfer to the outer ring atoms. A dynamical simulation of this effect certainly would be very interesting.

V. SUMMARY

Photodissociation experiments on small size-selected ionized helium clusters have been performed by measuring the absorption profiles and the kinetic energy release to both charged and neutral fragments. The results indicate that small He_n^+ clusters ($n=3$–7) consist of a charged linear symmetric trimer core, with further neutral atoms attached in equatorial ring positions. Starting from He_8^+ helium atoms are also placed near the ends of the trimer core, thus opening the possibility that at least for short times an isomer with a linear tetramer core structure is formed. This change in the ionic core results in a red shift of the absorption maximum from 5.3 to 5.0 eV and in the appearance of a different kinetic energy release pattern. The total binding energy of the He_3^+ was determined to be 2.6 ± 0.15 eV.

ACKNOWLEDGMENTS

We thank Jan Harms for help with the installation of the helium cluster source. This work has been partially supported by the Deutsche Forschungsgemeinschaft through SFB 276, TP C5.

[1] *Clusters of Atoms and Molecules, Bd. I+II*, edited by H. Haberland (Springer, Berlin, 1994).
[2] J. G. Maas, N. P. van Asselt, P. J. Nowak, J. Los, S. D. Peyerimhoff, and R. J. Bunker, Chem. Phys. **17**, 217 (1976).
[3] P. L. Patterson, J. Chem. Phys. **48**, 3625 (1968).
[4] H. Buchenau, J. Northby, E. L. Knuth, J. P. Toennies, and C. Winkler, J. Chem. Phys. **92**, 6875 (1990).
[5] H. Buchenau, J. P. Toennies, and J. A. Northby, J. Chem. Phys. **95**, 8134 (1991).
[6] R. Fröchtenicht, U. Henne, J. P. Toennies, A. Ding, Th. Drewello, and M. Fieber-Erdmann (unpublished).
[7] K. Balasubramanian, M. Z. Liao, and S. H. Lin, Chem. Phys. Lett. **142**, 349 (1987); J. Phys. Chem. **91**, 5836 (1987).
[8] M. Rosi and Ch. W. Bauschlicher, Chem. Phys. Lett. **159**, 479 (1989).
[9] J. Ackermann and H. Hogreve, Mol. Phys. **68**, 279 (1989).
[10] J. Ackermann and H. Hogreve, Chem. Phys. **157**, 75 (1991).
[11] V. Staemmler, Z. Phys. D **16**, 219 (1990).
[12] V. Staemmler, Z. Phys. D **22**, 741 (1992).
[13] H. Haberland, B. v. Issendorff, T. Kolar, H. Kornmeier, Ch. Ludewigt, and A. Risch, Phys. Rev. Lett. **67**, 3290 (1991).
[14] H. Haberland and B. v. Issendorff (unpublished).
[15] B. v. Issendorff, H. Haberland, R. Fröchtenicht, and J. P. Toennies, Chem. Phys. Lett. **233**, 23 (1995).
[16] H. Haberland, H. Kornmeier, C. Ludewigt, and A. Risch, Rev. Sci. Instrum. **62**, 2621 (1991).
[17] K. P. Huber and G. Herzberg, *Constants of Diatomic Molecules* (Van Nostrand Reinhold, New York, 1979).
[18] R. N. Zare, *Angular Momentum, Understanding Spatial Aspects in Chemistry and Physics* (Wiley, New York, 1988).
[19] B. v. Issendorff, Ph.D. thesis, University of Freiburg, Freiburg (1994).
[20] Z. Y. Chen, C. R. Albertoni, M. Hasewaga, R. Kuhn, and A. W. Castleman, J. Chem. Phys. **91**, 4019 (1989).
[21] T. Nagata, J. Hirokawa, T. Ikegami, and T. Kondow, Chem. Phys. Lett. **171**, 433 (1990).
[22] T. Ikegami, T. Kondow, and S. Iwata, J. Chem. Phys. **99**, 3589 (1993).
[23] If in the fragmentation of a rigidly linear He_3^+ the middle particle had more than half of the velocity of the faster one of the outer particles, momentum conservation would require that it has a higher velocity than the slower outer one, which is not possible.